Live Tissue Classification Using Real-time Thermography

Junren Ran†
Mechanical Engineering,
University of Illinois,
Urbana, IL.
jran2@illinois.edu

Yaswanth Sai Jetti†
Mechanical Engineering,
University of Illinois,
Urbana, IL.
yjetti2@illinois.edu

Adi Pasic†
Electrical and Computer Engineering,
University of Illinois,
Urbana, IL
pasic2@illinois.edu

***Abstract*—We develop a classifier to identify the tissue type using real-time thermography data during an electrosurgery. Firstly, we solve the Maxwell-Cattaneo hyperbolic differential equation for a wide range of thermal parameters: diffusivity (α) and relaxation time (τ) values. Then, we use the simulated data to train a convolution neural network (CNN) that predicts α and τ for a given thermal image. Subsequently, the thermography data is fed to the constructed CNN to obtain the approximate distributions of α and τ for liver and skin separately. These distributions are further used to generate sequential predictions by incorporating a naïve Bayes model. We demonstrated a relatively high accuracy of this classifier, which could be used for making control decisions with some caution.**

***Index Terms*—tissue classification, neural networks, naïve Bayes, non-Fourier heat conduction, neural differential equations**

I. Introduction

In the past decades, there has been an increase in the interest in robot-assisted surgery over conventional laparoscopy. To achieve automated surgery, the computer would need to make control decisions on its own. One of the most common surgery methods is electrosurgery, which accounts for half of the surgical procedures [1]. Electrosurgery uses Radiofrequency (RF) ablation to cut tissue and control bleeding in an operation. RF electrical currents pass through biological tissue to achieve controlled heating of desired region. During a surgery, providing the suitable power according to tissue type (i.e., muscle, liver, lung) is important for minimizing unnecessary damage. Therefore, identification of tissue type is an essential part of the automation of electrosurgery. The goal of this project is to create a method that can differentiate the tissue types during an electrosurgery process using their thermal responses from *in vivo* infrared thermography.

Fig. 1 shows an image taken during an electrosurgery procedure on porcine liver. The blue tip in the picture is the electrosurgery pencil. Fig. 2 is an example of the thermographer output during electrosurgery. These are Infrared images, which could be calibrated to represent the temperature field. The horizontal line on the bottom right side is the electrode and the diagonal "cone" in the center is the cut made by the electrode. We would like the computer to be able to "guess" the tissue type by looking at a sequence of these images.

† These authors contributed equally.

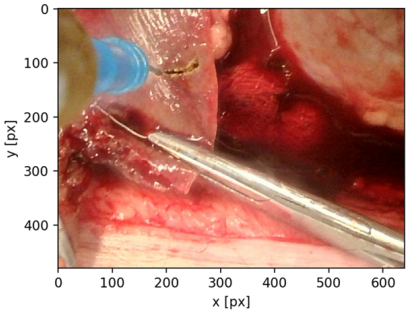

Fig. 1: Picture taken during electrosurgery

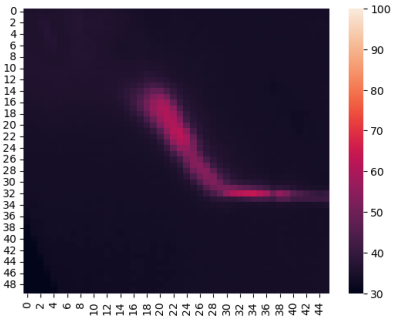

Fig. 2: An example of thermographer output during electrosurgery

In this paper, we are proposing a novel method that uses a Convolutional Neural Network (CNN), trained with numerical simulation, in combination with Naïve Bayes (NB) probability update to generate a real-time prediction of the tissue type that is being operated on using the thermographer output.

The flowchart of our overall solution strategy combing the CNN and NB model to get real-time predictions is shown in Fig. 3.

II. Data Visualization and Cleaning

In this study, we collected thermographer data of nine cuts in total on two types of porcine tissues during a live experiment as mentioned in Table I. We must note here that this is a very small data set. One of the challenges with using this

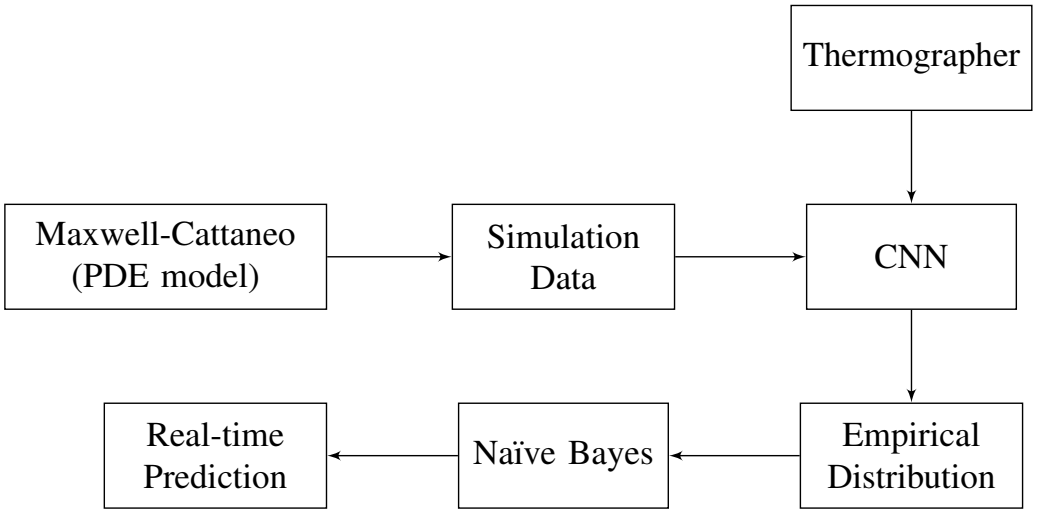

Fig. 3: Flowchart of the solution strategy

TABLE I: Data summary

	Cuts	Frames
Skin	4	194
Liver	5	129
Total	9	323

data is that the operating conditions for each cut may vary with respect to camera angle, heat intensity, and cut duration. Secondly, the accurate physical properties of the tissues that were operated on are not known; we only know the tissue type. During the surgery, the cuts are made in different directions so we can observe that the angle of cut varies from one cut to the other. Therefore, the portion of the image corresponding to the electrode should be processed and the the image should be appropriately rotated *a priori* in order to accurately classify the tissue type later. Fig. 4 shows an example of the thermographer output after a rough cleaning. We can see that the line of cut has been rotated so that it is close to being horizontal, the background had been shifted to zero and the majority of the electrode has been removed from the image, since the electrode is not part of the biological tissue. Then we performed a principal component analysis (PCA) to visualize this high-dimensional data in a low-dimensional space. The first and second principal components of the combined cut thermography data are shown in Fig. 5. We can see that the liver cut data and skin cut data can be clearly demarcated. This shows us that there are differences in the thermo-responses of different tissues and gives us hope that they could be differentiated in real-time.

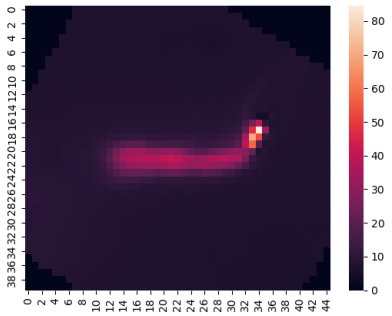

Fig. 4: Sample thermographer output after cleaning

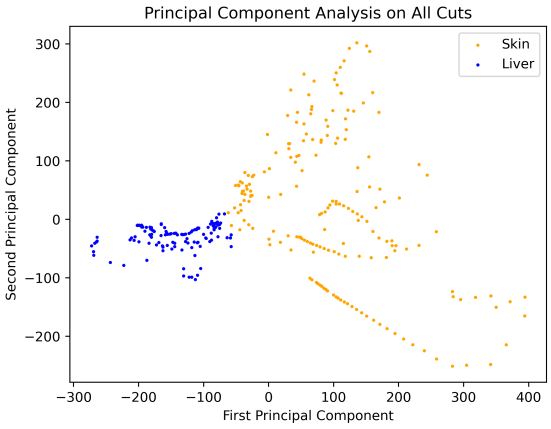

Fig. 5: The first and second principal components of thermography data of all the cuts

III. Heat Transfer Model

In order to build a better physics-based model, we need a deeper understanding of the underlying heat transfer process. By looking at the thermal images, we can see that the temperature profile in Fig. 2 seems to have a "cone-ish" outline, which reminds us of shock waves, or hyperbolic heat transfer. Therefore, we would like to use a non-Fourier type heat transfer model with a finite speed of propagation. One of the common non-Fourier heat transfer model is Maxwell-

Cattaneo [2], [3] governed by the following partial differential equation (PDE):

$$\frac{\partial \Theta}{\partial t} + \tau \frac{\partial^2 \Theta}{\partial t^2} = \alpha \nabla^2 \Theta$$

Here, Θ is temperature, t is time, τ corresponds to relaxation time, $\alpha = k/\rho c_p$ is the thermal diffusivity, where ρ is mass density and c_p is specific heat at constant pressure.

With this model, we would be able to numerically simulate an electrosurgery cut as a transient heat transfer process with a heat source (the electrode) moving horizontally across a domain (the biological tissue) with homogeneous Neumann boundary conditions. The Maxwell-Canttaneo equation could be solved using a second order finite-difference stencil in space and a Runge-Kutta scheme in time, details on the solver can be found in [4].

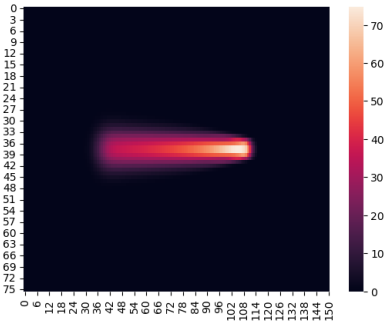

Fig. 6: Example of a numerical simulation result

Fig. 6 shows a sample frame in a numerical simulation solution from MATLAB, with a thermal diffusivity $\alpha = 0.0021 cm^2/s$ and relaxation time $\tau = 0.1s$. We can see that the temperature profile of the numerical solutions closely resemble the outputs from the thermographer during surgery processes. Our hope is that machine learning could be used to identity the physical parameters when a temperature profile is provided.

IV. Solution approach

With the numerical model show in the previous section, we are able to generate a large number of training data (limited by time and computing power). From literature [5], we learned that the thermal diffusivity of porcine skin and liver can range from about $\alpha = 0.0013 cm^2/s$ to $0.005 cm^2/s$. Since there is not much established data on relaxation time of porcine tissues, we estimate a range of $\tau = 0.1s$ to $0.25s$ from experience in combination with some published data [6]. In this study, as an example, we initially perform heat transfer simulations for 50 different combinations of α and τ to generate dynamic thermal response data that covers the range of thermal properties of the tissue types liver and skin. Then, we build a convolutional neural network and use these simulated dynamic thermal data to train the CNN model as discussed below. Furthermore, this neural network model is used to predict the two thermal parameters on the experimental data. Later, a naïve Bayes model is employed to predict the likelihood of the organ that is being operated up on in real-time.

A. Convolution neural network

We would like to train a neural network model that can identify these parameters when a thermo-image is given. Since our experimental data contains a lot of noise and the physical properties of the tissues that were operated on are not clearly labeled, we only know the tissue type instead of the exact numbers, we decided that it is better to use numerical simulation results to train our neural network. We can simulate the solution to the PDE in Eq. III with a range of α and τ pairs, since these two parameters are about 100 times different in magnitude, we will first normalize them before training and convert back to the actual value afterwards.

Then, we built a convolutional neural network using the PyTorch package [7] in Python and trained it with our simulation data. Fig. 7 below shows the layout of our convolutional neural network model. Each observation would first be passed through two convolutional and max-pool layers and then flattened. After that, the flattened array would pass through three linear dense layers, with 21, 120, and 60 nodes, that turns the flattened data to the two final outputs, prediction of α and τ. (dense layers are not shown in the figure). The mean square error is used as the loss function in optimization. Once we have a neural network that is capable of estimating the heat transfer parameters when a frame is provided, we can then feed the outputs from a sequence of frames in to the naïve Bayes model.

B. Naïve Bayes model

We form a naïve Bayes model with the features: Organ type (O), and all the thermal parameter data corresponding to the image frames is indicated by F_t with $t = 1, 2, 3, ..., T-1, T$. The variable O takes two values: liver (L) and skin (S). Each F_t has two variables: α_t and τ_t, which are computed using the neural network. The naïve Bayes model for obtaining the likelihood of the organ being operated up on till time t is given below:

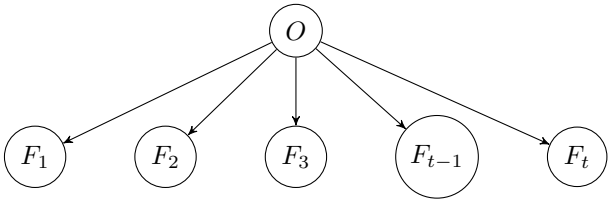

$$P(F_t|O) = P(\alpha_t|O)P(\tau_t|O)$$

$$P(O = L) = P(O = S) = 0.5$$

For instance, the conditional probability $P(O = L|F_t)$ is calculated as follows:

$$P(O = L|F_1, ..., F_t) \propto P(F_t|O = L)P(O = L|F_1, ..., F_{t-1})$$

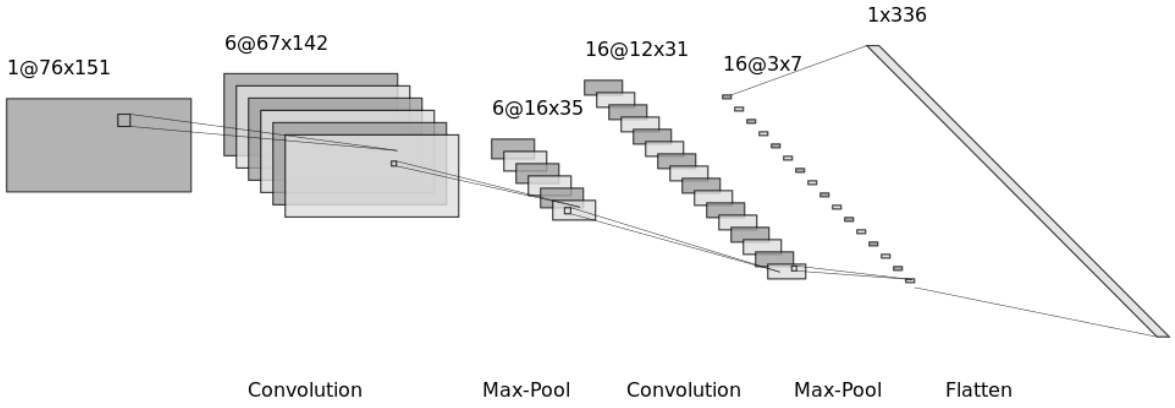

Fig. 7: Convolutional neural network diagram

Note that $P(F_t|O) = P(\alpha_t|O)P(\tau_t|O)$ since α_t and τ_t are independent. The node F_{t+1} will be added to the above model as we obtain the new frame to obtain the updated likelihood. Conditional probabilities ($P(F_t|O)$) are approximated after applying the neural network to the experimental data (thermographer outputs).

V. Results and Discussion

A. Neural network predictions on real data

The histograms of α and τ paramters obtained from the convolution neural network for liver and skin cuts are shown in Fig. 8. We approximate these to be Gaussian distributions and numerically fit the data to obtain mean and standard deviation. The approximated normal distributions are shown in the insets of the corresponding plots (see Fig. 8). We notice that the mean values of α and τ for liver and skin cuts are distinct. As mentioned above, these distributions will be used while evaluating $P(\alpha_t|O)$ and $P(\tau_t|O)$.

B. Real-time prediction on liver cuts

The real-time tissue classifier starts with the prior probabilities of 0.5 for the liver and skin. As more and more frames are added, the probability of the organ being operated upon is updated. This dynamic progression of probabilities for all the liver cuts is shown in Fig. 9. By the time all the frames are evaluated, the classifier correctly identifies four out of the five cuts as belonging to liver. If we look closely at the cut which was incorrectly predicted (Liver cut 4), we observe that the classifier identified the tissue correctly as liver till the time the last frame was added. It is only when the last frame was added, that the prediction abruptly changed to skin. This shows that the model is susceptible to abrupt changes in prediction with just an addition of a bad frame. There might be various reasons for deeming a frame bad - sudden camera movement, blood drainage out of the cut etc. On the other hand, the prediction for the Liver Cut 5 was varying between liver and skin during the cut. Therefore, there is a need for improving the prediction model over just using the updated probability values obtained at the last frame.

C. Real-time prediction on skin cuts

As with the predictions for skin cuts, the real-time tissue classifier starts with the prior probabilities of 0.5 for the liver and skin. The dynamic progression of probabilities for all the liver cuts is shown in Fig. 10. By the time all the frames are evaluated, the classifier correctly identifies all four cuts as belonging to skin. However, like for the case of liver cuts, these predictions should be further investigated. For instance, if we look at the case of Skin cut 1, the classifier predicts the tissue to be liver for most of the time and it switches to predicting liver only during the last frames. We observe a similar prediction behavior for the Skin cut 2. It would be better if a variable learning rate is used in making the predictions. In the beginning of the cuts, the temperature profiles should all look very similar to each other, since they are all just a blob. As the cuts progress, the outlines of the "cones" would get clearer. Therefore, when making the control decisions, our confidence in the earlier frames should be lower and the later frames should be higher.

VI. Conclusions

In this work, we developed a classifier to identify the tissue type using the real-time thermography data that could potentially be used in automated electrosurgery. To begin with, we solve the Maxwell-Cattaneo hyperbolic differential equation numerically for a wide range of thermal diffusivity (α) and relaxation time (τ) values over a two-dimensional domain. Subsequently, we use the simulated data to train a convolutional neural network that predicts α and τ for a given thermal image. Then, the thermographer data during surgery is fed to the constructed CNN to obtain the approximate distributions of α and τ for liver and skin separately. These

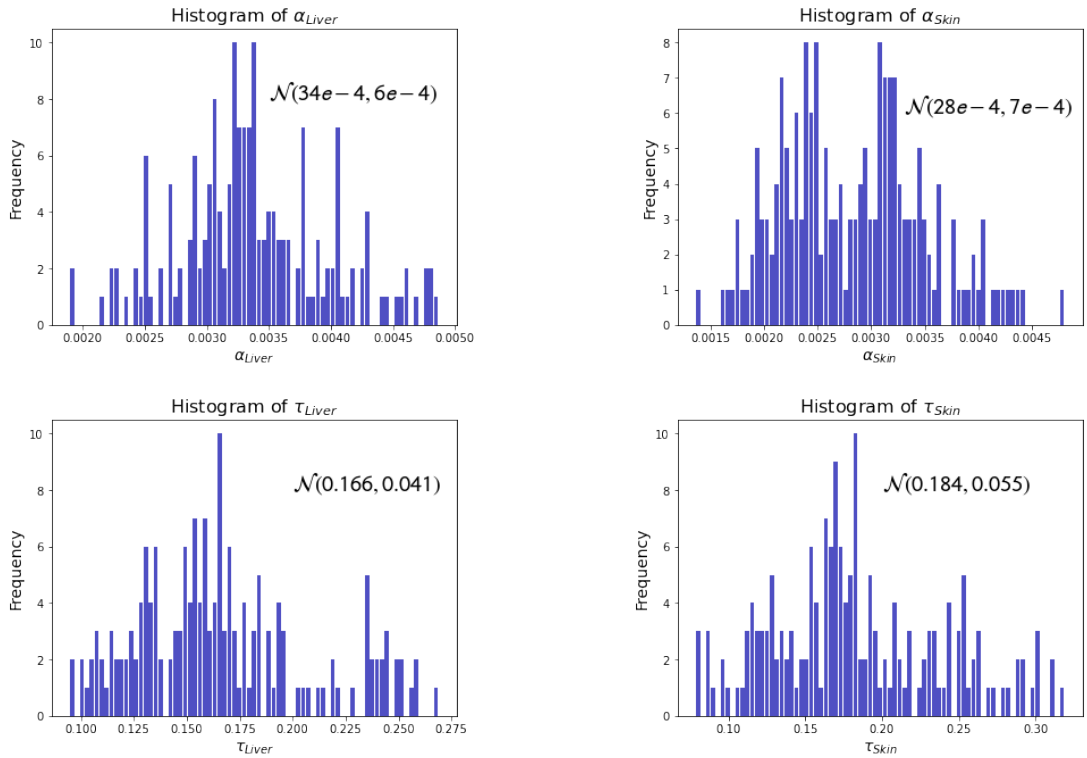

Fig. 8: Distributions of α and τ for liver and skin obtained using Neural network

distributions are further used to generate sequential predictions for the probability of tissue type by incorporating a naïve Bayes model. We demonstrated a relatively high accuracy of this classifier, with some caveats.

We observed that a bad frame can abruptly change the prediction. We also noticed that the thermography data obtained towards the end of a cut could have a great influence on the predictions if we only look at the final probability. Therefore, the naïve Bayes prediction could be augmented by assigning a confidence level (learning rate) to each frame, to reduce the effect of bad frames and abrupt changes when making control decisions during surgery. The present model does not capture dependencies through time between successive frames. A recurrent neural network trained to classify tissue type directly might resolve some of these limitations. Moreover, the approximate distributions are obtained by feeding the entire real data to the neural network and the final predictions are made on the same data owing to having a very small data set. Therefore, there is an inter-dependency between the prediction and the model, which is not desirable. Ideally, we would infer the distribution of the thermal parameters on a large number of experimental data for a more accurate description (more experiments required). Currently, the model is only capable of classifying two types of tissues (porcine skin/liver). In the future, the model could be expanded to more organs (tissue types).

ACKNOWLEDGEMENT

Experimental data reported in this publication was provided by the Bentsman group at UIUC, supported by the National Institute of Biomedical Imaging and Bioengineering of the National Institutes of Health under award number R01EB029766. The content is solely the responsibility of the authors and does not necessarily represent the official views of the National Institutes of Health. We would like to thank Hamza El-Kebir for gathering the experimental data.

REFERENCES

[1] D. Palanker, A. Vankov, and P. Jayaraman, “On mechanisms of interaction in electrosurgery”, New Journal of Physics, vol. 10, no. 12, p. 123022, Dec. 2008.

[2] J. Ignaczak, and M. Ostoja-Starzewski, “Thermoelasticity with Finite Wave Speeds”, Oxford Mathematical Monographs, Oxford Academic. Oxford, Feb. 2010.

[3] C. Cattaneo, “Sulla conduzione de calore”, Atti Sem Mat Fis Modena, vol. 3, p. 83–101, 1948.

[4] J. Ran, M. Ostoja-Starzewski, Y. Povstenko, “Mach Fronts in Random Media with Fractal and Hurst Effects,” Fractal Fract, vol. 5, p. 229, 2021.

[5] D. Francis, “Physical-Properties-of-Tissues A Comprehensive Reference Book”, Academic Press, 1990.

[6] A. Madhukar, Y. Park, W. Kim, H.J. Sunaryanto, R. Berlin, L.P. Chamorro et al. “Heat conduction in porcine muscle and blood: experiments and time-fractional telegraph equation model”, J. R. Soc. Interface 16, 2019.

[7] A. Paszke, S. Gross, F. Massa, A. Lerer, J. Bradbury, G. Chanan et al. “PyTorch: An Imperative Style, High-Performance Deep Learning Library”, In Advances in Neural Information Processing Systems, vol. 32, p. 8024–8035, 2019.

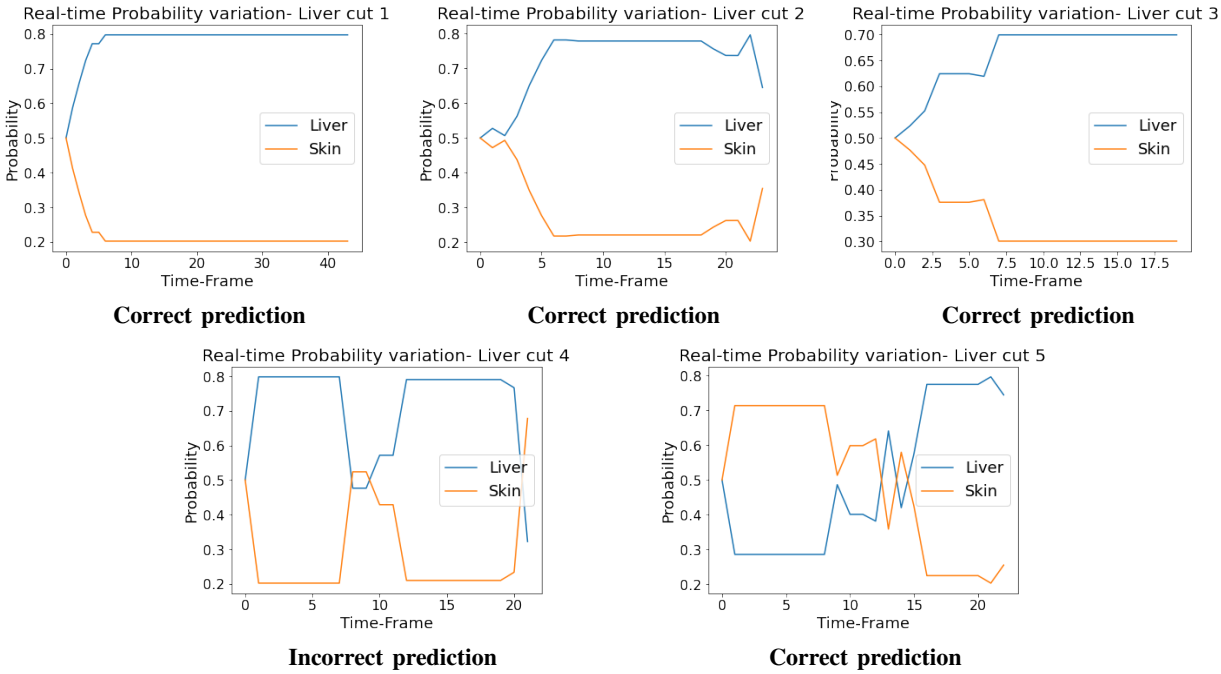

Fig. 9: Real-time prediction on liver cuts

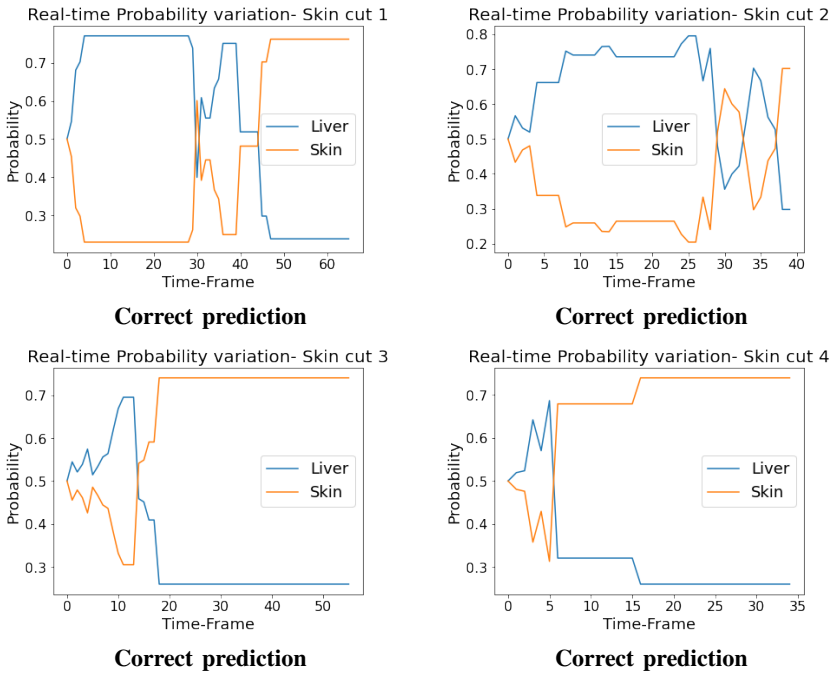

Fig. 10: Real-time prediction on skin cuts